Unconventional wave reflection due to "resonant surface"

Logan Schwann, Claude Boutin

Unconventional wave reflection due to "resonant surface"

L. Schwan, C. Boutin *

Université de Lyon, Ecole Nationale des Travaux Publics de l'Etat, LGCB, UMR CNRS 5513, CeLyA, Rue Maurice Audin, 69518 Vaulx-en-Velin, France

HIGHLIGHTS

- A drastic change of *P* and *SV* waves conversion.
- The full depolarization of normally-incident shear waves.
- The conversion of *SH* waves into *P* and *SV* waves.
- The possibility of the whole reflected field to vanish.

Keywords:
Wave reflection
Resonant surface
Surface impedance
Depolarization
Boundary layer
Homogenization

ABSTRACT

This study deals with the reflection phenomena in an elastic half-space on which lies a "resonant surface". The resonant surface consists in a 2D periodic repetition of a surface element over which linear oscillators are distributed. Following the homogenization approach developed by Boutin and Roussillon (2006) [1], the periodic distribution of oscillators (1 to 3D sprung-mass) is reduced to a frequency-dependent surface impedance. It is hereby shown that the surface motion comes to zero in the resonating direction around the oscillators' eigenfrequency. Further, the surface impedance may be isotropic or anisotropic, according to the type of oscillator. Thereby unusual free/rigid mixed boundary condition arises, which in turn induces atypical reflected wave fields. The most notable effects are (i) drastic change of *P* and *SV* waves conversion, (ii) depolarization of shear waves, (iii) conversion of *SH* waves into *P* and *SV* waves, and (iv) possibility of vanishment of the whole reflected field. The physical insight of the theoretical results is discussed and numerical illustrations are provided.

1. Introduction

The present study is concerned with the reflection phenomena in an elastic homogeneous half-space on which lies a "resonant surface". The resonant surface consists in linear oscillators distributed on the "free" surface with sufficient regularity to consider that the "oscillator layer" is characterized by a representative surface element (RSE) containing a few oscillators.

The simplest realization of this situation is a 2D periodic repetition of the same representative surface element Σ over which linear oscillators are distributed (Fig. 1). Such specific configurations are encountered in different domains of application and at different scales, according to the nature of the oscillators and of the supporting medium: for instance in geophysics, when considering the skyscraper-city effect on seismic motions e.g. [2–4]; in ultrasound survey, when inverting signals in the presence of highly corrugated surface; in dynamics of nanostructures, with nanotubes or nanocrystals equidistantly grown on the substrate [5].

* Corresponding author.
E-mail addresses: logan.schwan@entpe.fr (L. Schwan), claude.boutin@entpe.fr (C. Boutin).

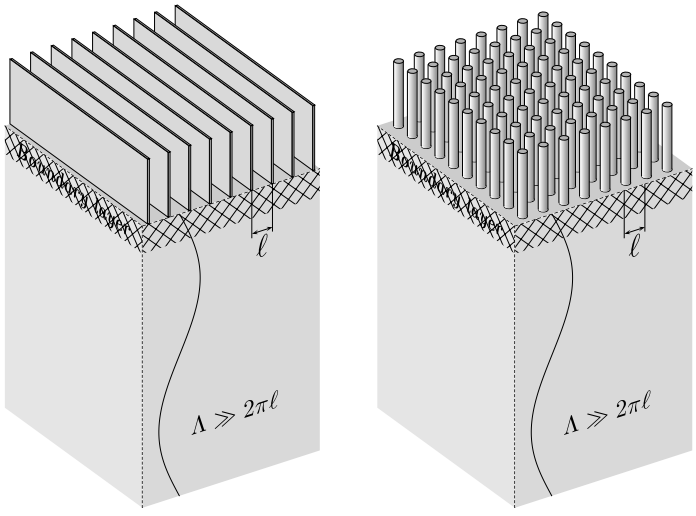

Fig. 1. Basic examples of resonating surface.

We address long wave propagation in the sense that the wave-lengths in the media are much larger than the size of the period (or of the RSE). In other words, a scale-separation condition is satisfied. The key point of the study is to assume that the resonance of the oscillators occurs within the scale-separation frequency range.

In this framework, the paper [1] demonstrates theoretically through multiple scale homogenization method [6,7] that the resonant surface can be described at the leading order by an equivalent boundary condition. This latter is formulated as a macroscopic impedance condition which frequency-dependent expression is directly related to the features of the oscillator.

The aim of the present paper is to systematically investigate the unusual effects related to the resonance of the oscillators and to evidence how much the reflected field differs from the field reflected with a free surface or with a rigid upper-layer configuration. For simplicity, we consider a single oscillator on the period, with three degrees of freedom associated to the horizontal or vertical directions. Isotropic (resp. anisotropic) horizontally resonant surface is obtained when the oscillator presents the same (resp. different) features in both horizontal directions. This simple situation underlines the key aspects of the phenomena, that can be extended with similar principles to more complex cases.

The paper is organized as follows. In Section 2, the basic assumptions and essential aspects of the modeling of a resonant surface by an equivalent impedance are briefly recalled. In Section 3, a general formulation of the wave reflection in presence of a surface impedance is proposed. Section 4 is devoted to the effect of isotropic horizontally resonant surfaces on the reflection of incident *SH*, *SV* and *P* plane waves. Sections 5 and 6 deal with the same questions for vertically resonant surfaces and anisotropic horizontally resonant surfaces.

2. Equivalent impedance of a "resonant surface"

This section sums up the principles governing the theoretical derivation of the equivalent impedance of a resonant surface (for more details see [1]).

2.1. Statement of the boundary layer problem

Consider a Σ-periodic distribution of linear oscillators lying on top plane surface Γ (of outward normal $\mathbf{n}$) of a homogeneous isotropic half-space of elastic tensor $\mathbf{C}$ (Lamé coefficients λ, μ) and density ρ. In this linear system, we study the propagation of harmonic waves of frequency $f = \omega/2\pi$, assuming a scale separation between the characteristic size ℓ of Σ ($\ell = O(\sqrt{|\Sigma|})$) and the shear wavelength Λ in the medium, thus:

$$\varepsilon = 2\pi\ell/\Lambda \ll 1 \quad \text{where } \Lambda = \frac{2\pi c_S}{\omega},\ c_S = \sqrt{\frac{\mu}{\rho}}. \tag{1}$$

The oscillators set in motion by the waves induce on Γ a heterogeneous distribution of stresses, $\sigma.\mathbf{n} = \mathbf{t}\exp[-i\omega t]$ (in the sequel the term $\exp[-i\omega t]$ is systematically omitted). Because of periodicity and scale separation, (i) at the micro-scale, $\mathbf{t}$ is locally Σ-periodic, (ii) the distribution $\mathbf{t}$ also varies at the wavelength scale. The local 2D periodicity of $\mathbf{t}$ enforces the same 2D periodicity of the micro-scale perturbations of the physical quantities in the medium. Furthermore, as the sources of micro-variations are located on Γ, it is inferred that away from Γ small scale variations vanish, while macro-variations remain. Such a situation corresponds to a boundary layer located in the vicinity of the surface (see also in other contexts [6,8]).

2.2. Derivation of the equivalent surface impedance through homogenization

To handle this two scales phenomenon, macro-variables $\mathbf{x}$ and micro-variables $\mathbf{y} = \varepsilon^{-1}\mathbf{x}$ are introduced. In accordance with the above analysis:

- away from the surface, the waves propagate as macroscopic fields described by the macro-variable $\mathbf{x}$. The relevant boundary conditions on Γ are a priori unknown for the macro-field;
- in the vicinity of the surface, a boundary layer field varying at both micro and macro-scale superposes the macro-field. The stress distribution $\mathbf{t}$ exerted by the oscillators on Γ is balanced by the total field, i.e. the macroscopic and the boundary layer fields.

Then, the formal developments (not presented here) follow the usual homogenization method [6]. The missed boundary condition for the macro-field is derived from the global equilibrium of the periodic boundary layer. It shows that the macro-field balances the *mean* surface stresses $\frac{1}{|\Sigma|}\int_\Sigma \mathbf{t}\mathrm{d}s = \mathbf{T}$. Further, since the linear oscillators respond to the surface motion, the macro-stress $\mathbf{T}$ on Γ is related to the surface velocity $-i\omega\mathbf{U}_\Gamma$ through a frequency-dependent impedance matrix $\mathbf{Z}_\Gamma$ defined by the properties of the oscillators.

Finally, the leading order description is fully determined by the macro-field $\mathbf{U}(\mathbf{x})$ governed by the elastodynamic equation of the elastic media (2) and the boundary condition (3) stating that the "oscillators layer" at the leading order acts as an equivalent impedance symmetric matrix (such formulation is also used in deterministic theory [9], in fuzzy structure probabilistic approach [10,11] and in electromagnetics [12]):

$$\mathbf{div}[\mathbf{C} : \mathbf{e}(\mathbf{U})] = -\rho\omega^2\mathbf{U} \tag{2}$$

$$[\mathbf{C} : \mathbf{e}(\mathbf{U})].\mathbf{n} = -i\omega\mathbf{Z}_\Gamma.\mathbf{U} \quad \text{on } \Gamma. \tag{3}$$

Note that, at the leading order considered here, the surface motion is uniform on the period and the macro-field balances the *mean* surface stresses. Thus, possible effects of rotation and momentum induced by oscillator are negligible at this order, and appear as first order correctors (see [1]).

In the mathematical process, ε is an infinitesimal quantity that allows to solve the problems separately at different orders. This idealization is not reached in practice because both micro and macro-scale are finite. Consequently, the actual physical value of ε is a small but finite quantity, and the leading order description is correct up to the precision ε only.

2.3. A basic example

Conversely to impedance of elastic media, $\mathbf{Z}_\Gamma$ varies with frequency. To illustrate this key property, consider for simplicity a single oscillator located on Σ (situations with a finite number of oscillators n, of different impedances orientated in various directions, would lead to $\mathbf{Z}_\Gamma = \sum_n \mathbf{Z}_{\Gamma_n}$). This oscillator presents a single degree-of-freedom characterized by a stiffness k, a viscous damping coefficient c and a mass m in a given direction (e.g. horizontal) so that, focusing on this direction, the problem is scalar.

The harmonic macroscopic surface motion U_Γ induces a motion U_m of the mass of the oscillator. The force $|\Sigma|T$ imposed by the oscillator on Γ balances the mass inertia. Consequently

$$|\Sigma|T = (k - i\omega c)(U_m - U_\Gamma) = m\omega^2 U_m.$$

Then, introducing the eigenfrequency $f_o = \omega_o/2\pi$ and the damping ratio ξ (in the sequel, weak damping is assumed)

$$\omega_o = 2\pi f_o = \sqrt{k/m}; \qquad \xi = c/2\sqrt{km} \ll 1$$

we have

$$\frac{U_m}{U_\Gamma} = \frac{1 - 2i\xi\frac{\omega}{\omega_o}}{1 - 2i\xi\frac{\omega}{\omega_o} - \frac{\omega^2}{\omega_o^2}}; \qquad T = \frac{m\omega^2}{|\Sigma|}\frac{1 - 2i\xi\frac{\omega}{\omega_o}}{1 - 2i\xi\frac{\omega}{\omega_o} - \frac{\omega^2}{\omega_o^2}}\,U_\Gamma = -i\omega Z_\Gamma U_\Gamma. \tag{4}$$

This last relation provides the impedance Z_Γ (in the oscillator direction). Normalized by the shear impedance $Z = \sqrt{\rho\mu} = \rho c_S$ of the elastic half-space, Z_Γ is the product of a constant parameter η and of a dimensionless dynamical function (see Fig. 2):

$$\frac{Z_\Gamma}{Z} = -\eta\frac{\left(-i\frac{\omega}{\omega_o}\right)\left(1 - i2\xi\frac{\omega}{\omega_o}\right)}{1 - i2\xi\frac{\omega}{\omega_o} - \frac{\omega^2}{\omega_o^2}} \quad \text{where } \eta = \frac{\omega_o\ell}{c_S}\frac{m}{\rho|\Sigma|\ell}. \tag{5}$$

2.4. Features of resonant surfaces

Parameter η is made up of two terms: the first one $\varepsilon_o = \omega_o\ell/c_S$ is the scale ratio at the eigenpulsation ω_o of the oscillator. For the resonance to occur under scale separation condition, $\varepsilon_o \ll 1$. The second term is the ratio between the oscillator

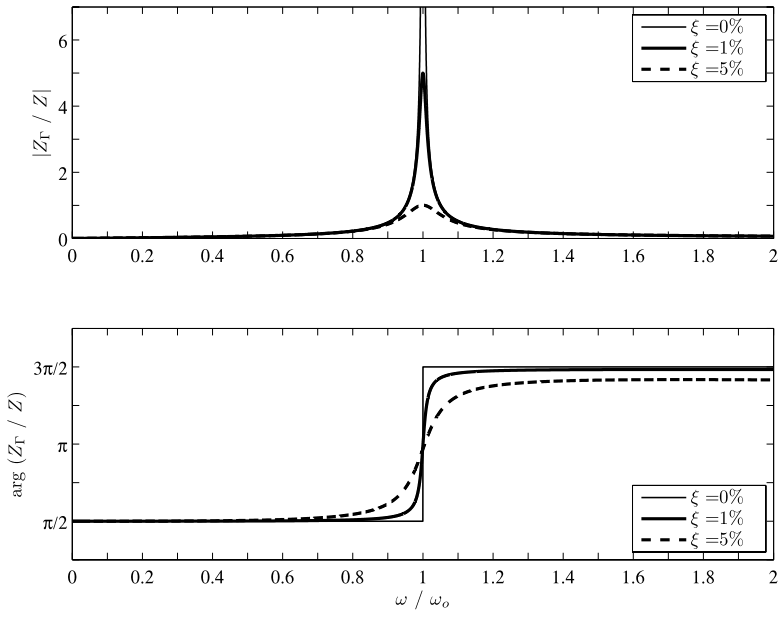

Fig. 2. Ratio between the surface impedance Z_Γ in the direction of oscillations and the shear impedance Z of the medium versus dimensionless frequency. Calculations performed with $\eta = 0.1$ for different values of oscillator damping.

mass m and the mass $M_\Sigma = \rho|\Sigma|\ell$ of the medium under one period Σ on a depth ℓ. As a consequence, η is at best of the first order (in ε_o) if the resonating mass m is of the same order as M_Σ.

Combining the order of magnitude of η and the asymptotic behaviors of the dimensionless dynamical function enables to estimate the impedance ratio Z_Γ/Z, hence the boundary conditions equivalent to the oscillators, in the low, high and resonant frequency ranges.

$$\left|\frac{Z_\Gamma}{Z}\right| \underset{\omega\ll\omega_0}{\simeq} \left|i\frac{\omega}{\omega_0}\eta\right| \ll 1; \qquad \left|\frac{Z_\Gamma}{Z}\right| \underset{\omega\gg\omega_0}{\simeq} |-2\xi\eta| \ll 1; \qquad \left|\frac{Z_\Gamma}{Z}\right| \underset{\omega\to\omega_0}{\simeq} \left|-\frac{\eta}{2\xi}\right|. \tag{6}$$

In quasi static ($\omega \ll \omega_o$) or inertial ($\omega \gg \omega_o$) regime, the impedance Z_Γ is much smaller than the impedance of the medium Z. Consequently, the boundary condition tends to the free surface condition.

Conversely, at the resonance of a weakly-damped oscillator ($\xi \ll 1, \omega \to \omega_o$) the impedances ratio tends to $-\eta/2\xi$. If the oscillators are perfectly elastic ($\xi = 0$), Z_Γ/Z becomes infinite, and the surface displacement tends to zero in the direction of the oscillations: this phenomenon has the same effects as a rigid condition (in the direction of the oscillations only). In the sequel, this situation will be referred conveniently as "rigid" condition (despite differences between physical causes). Note also that Z_Γ is purely imaginary at any frequency when $\xi = 0$.

In practice, for the resonant surface effect to be not negligible at the resonance under the scale separation condition, the two following inequalities have to be fulfilled necessarily: $\varepsilon_o < 1$ and $\eta/2\xi > \varepsilon_o$. This provides the two following constrains for the oscillator:

$$k < \frac{m}{M_\Sigma}\mu\ell; \quad m > 2\xi M_\Sigma.$$

In the following, numerical applications will be performed considering $\eta = 10\%$ and either elastic oscillator $\xi = 0$ or damped oscillator $\xi = 1\%$ or $\xi = 5\%$.

To sum up, a resonant surface is a "device" that enables to switch from quasi-free surface condition to quasi-rigid surface condition in the resonance frequency range and in the resonance direction only. Combining oscillators with different direction of oscillations open the possibility of unusual boundary condition mixing free and rigid conditions. Such situations, impossible to reach with an elastic upper layer, drastically change the usual reflection rules as detailed in the next sections.

3. Reflection with surface impedance. General formulation

We address here the reflection, in an isotropic half-space, of harmonic incident plane waves in presence of a surface impedance. For generality purpose, the eigenaxis of the symmetric matrix impedance $\mathbf{Z}_\Gamma$ are not specified. Thus, an incident plane wave $\mathbf{u}^I$ may give rise to a reflected field constituted by SH, SV and P plane waves ($\mathbf{u}^{SH_r}$; $\mathbf{u}^{SV_r}$; $\mathbf{u}^{P_r}$) in order to respect the boundary condition (3) on Γ ($\mathbf{n} = -\mathbf{e}_3$):

$$\left[\mathbf{C} : \mathbf{e}(\mathbf{u}^I + \mathbf{u}^{SH_r} + \mathbf{u}^{SV_r} + \mathbf{u}^{P_r})\right].\mathbf{e}_3 = i\omega\mathbf{Z}_\Gamma.(\mathbf{u}^I + \mathbf{u}^{SH_r} + \mathbf{u}^{SV_r} + \mathbf{u}^{P_r}). \tag{7}$$

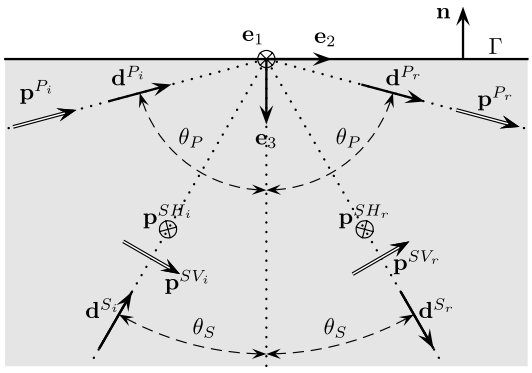

Fig. 3. Propagation and polarization convention of the plane waves.

Recall that the polarization of P and SV waves belongs to the incidence plane $\mathcal{P}$ – defined by the normal on Γ and the propagation vector of the incident (and reflected) wave – while SH wave polarization is orthogonal to $\mathcal{P}$. In the sequel, the reference basis $(\mathbf{e}_j, j = 1, 2, 3)$ is oriented as follows: $(\mathbf{e}_1, \mathbf{e}_2)$ are the in-plane directions of Γ; $\mathbf{e}_3 = -\mathbf{n}$ is the downward vertical direction; $(\mathbf{e}_2, \mathbf{e}_3)$ define the incident plane (see Fig. 3).

3.1. Description of wave fields

The field of motion of P or S plane waves (incident or reflected) takes the generic form in the basis $(\mathbf{e}_j)$:

$$\mathbf{u} = U\mathbf{p}\exp\left(i\frac{\omega}{c}\mathbf{d}.\mathbf{x}\right); \quad \mathbf{d} = d_2\mathbf{e}_2 + d_3\mathbf{e}_3 \tag{8}$$

where $U, c, \mathbf{p}, \mathbf{d}$ stand respectively for the complex amplitude, the wave velocity, the polarization vector and the propagation vector. Classically, both vectors are unitary in the sense of the scalar product, i.e. $\mathbf{d}.\mathbf{d} = \mathbf{p}.\mathbf{p} = 1$; they are real or complex for homogeneous or inhomogeneous waves. The incident wave is taken homogeneous, thus $d_2^I = \sin(\theta^I)$, $d_3^I = -\cos(\theta^I)$, where $\theta^I > 0$ is the incidence angle. Remind that for P waves $c = c_P = \sqrt{(\lambda + 2\mu)/\rho}$ and $\mathbf{p}^P$ is parallel to $\mathbf{d}^P$; for S waves $c = c_S = \sqrt{\mu/\rho}$ and $\mathbf{d}^S.\mathbf{p}^S = 0$. More precisely, we adopt the following convention for the polarization vectors of the incident and reflected waves (see Fig. 3):

$$\mathbf{p}^P = \mathbf{d}^P; \qquad \mathbf{p}^{SH} = \mathbf{e}_1; \qquad \mathbf{p}^{SV} = \mathbf{d}^{SV} \times \mathbf{e}_1 \mathrm{sgn}(\mathbf{e}_3.\mathbf{d}^{SV}) \quad \text{so that } p_2^{SV} > 0.$$

To satisfy the boundary conditions, all reflected plane waves have the same horizontal wave number d_2/c as the incident wave, i.e. d_2^I/c_I (Snell–Descartes law). We then deduce the propagation vectors:

$$\frac{d_2}{c} = \frac{d_2^I}{c_I}; \qquad d_3 = \pm\sqrt{1 - d_2^2} = \pm\sqrt{1 - \left(\frac{c}{c_I}d_2^I\right)^2}.$$

The signs $+$ and $-$ apply respectively for reflected and incident wave, and $\sqrt{a} = +i\sqrt{|a|}$ for $a < 0$ (shear waves with angle of incidence beyond the critical angle defined by $\sin(\theta_c^I) = c_S/c_P$ gives rise to inhomogeneous reflected P wave).

3.2. Surface stresses

The stress tensor is calculated from the isotropic elastic behavior:

$$\mathbf{C} : \mathbf{e}(\mathbf{u}) = \lambda \mathrm{div}(\mathbf{u})\mathbf{I} + 2\mu\mathbf{e}(\mathbf{u}).$$

Noticing that for any type of plane wave as defined by (8):

$$\mathbf{e}(\mathbf{u}) = \frac{i\omega U}{c}\frac{1}{2}(\mathbf{p}\otimes\mathbf{d} + \mathbf{d}\otimes\mathbf{p})\exp\left(i\frac{\omega}{c}\mathbf{d}.\mathbf{x}\right); \qquad \mathrm{div}(\mathbf{u}) = \frac{i\omega U}{c}\mathbf{p}.\mathbf{d}\exp\left(i\frac{\omega}{c}\mathbf{d}.\mathbf{x}\right)$$

the stress vector $[\mathbf{C} : \mathbf{e}(\mathbf{u})].\mathbf{e}_3$ on $\Gamma(x_3 = 0)$ is given by:

$$\boldsymbol{\sigma}\exp\left(i\frac{\omega}{c}d_2x_2\right) = \frac{i\omega U}{c}\left\{\lambda(\mathbf{p}.\mathbf{d})\mathbf{e}_3 + \mu(\mathbf{d}.\mathbf{e}_3)\mathbf{p} + \mu(\mathbf{p}.\mathbf{e}_3)\mathbf{d}\right\}\exp\left(i\frac{\omega}{c}d_2x_2\right).$$

Snell–Descartes law imposes identical spatial variations along the surface for all the waves. For expressing the boundary condition, it is then sufficient to determine the vector $\boldsymbol{\sigma}$ for the SH, SV and P waves by specifying $\mathbf{p}$ and $\mathbf{d}$ for each of them. With evident notations, using the shear impedance $Z = \mu/c_s = \sqrt{\mu\rho}$, we obtain:

$$\boldsymbol{\sigma}^a = i\omega U^a Z\mathbf{q}^a; \quad a = SH,\ SV,\ P$$

where the vectors of surface stress direction $\mathbf{q}^{SH}$, $\mathbf{q}^{SV}$ and $\mathbf{q}^P$ read:

$$\mathbf{q}^{SH} = d_3^{SH}\mathbf{e}_1; \qquad \mathbf{q}^{SV} = d_3^{SV}\mathbf{p}^{SV} + p_3^{SV}\mathbf{d}^{SV}; \qquad \mathbf{q}^P = \frac{c_S}{c_P}\left(2d_3^P\mathbf{d}^P + \left((\frac{c_P}{c_S})^2 - 2\right)\mathbf{e}_3\right).$$

3.3. Matrix formulation of the boundary condition

Now, consider (i) the (3×3) matrices $\mathbf{P}^r$, $\mathbf{Q}^r$, whose columns are respectively the vectors $\mathbf{p}$ and $\mathbf{q}$ of the reflected *SH*, *SV* and *P* waves, and (ii) the unicolumn matrix $[\mathcal{U}^r]$ of their amplitude:

$$\mathbf{Q}^r = [\mathbf{q}^{SH_r}, \mathbf{q}^{SV_r}, \mathbf{q}^{P_r}]; \qquad \mathbf{P}^r = [\mathbf{p}^{SH_r}, \mathbf{p}^{SV_r}, \mathbf{p}^{P_r}]; \qquad [\mathcal{U}^r] = {}^t[U^{SH_r}, U^{SV_r}, U^{P_r}].$$

With the adopted convention for polarization, their classic expression in the basis $(\mathbf{e}_j)$ is:

$$\mathbf{P}^r = \begin{bmatrix} 1 & 0 & 0 \\ 0 & d_3^{SV_r} & d_2^{P_r} \\ 0 & -d_2^{SV_r} & d_3^{P_r} \end{bmatrix}; \qquad \mathbf{Q}^r = \begin{bmatrix} d_3^{SH_r} & 0 & 0 \\ 0 & 1-2(d_2^{SV_r})^2 & 2\dfrac{c_S}{c_P} d_2^{P_r} d_3^{P_r} \\ 0 & -2d_2^{SV_r} d_3^{SV_r} & \dfrac{c_P}{c_S}\left(1-2\left(\dfrac{c_S}{c_P} d_2^{P_r}\right)^2\right) \end{bmatrix}. \tag{9}$$

Note that the unicolumn matrix $\mathbf{E}^1 = {}^t[1^{SH}, 0^{SV}, 0^{P}]$ is a common eigenvector of $\mathbf{P}^r$ and $\mathbf{Q}^r$, (with eigenvalues 1 and $d_3^{SH_r}$ respectively).

With these notations, the boundary condition (7) simplifies in the following form:

$$Z(\mathbf{q}^I U^I + \mathbf{Q}^{\mathbf{r}}[\mathcal{U}^r]) = \mathbf{Z}_\Gamma.(\mathbf{p}^I U^I + \mathbf{P}^{\mathbf{r}}[\mathcal{U}r]).$$

Introduce similarly the matrices $\mathbf{P}^i$, $\mathbf{Q}^i$ built in the same manner as $\mathbf{P}^r$, $\mathbf{Q}^r$ (replacing index r by i, all vectors being defined from the same horizontal wave number d_2/c). Because of the symmetry between incident and reflected fields of the same mode and the chosen convention on *SV* polarization, $(p_2^{SV_r} = p_2^{SV_i})$, we have:

$$\mathbf{P}^i = \mathbf{I}^* \mathbf{P}^r; \qquad \mathbf{Q}^i = -\mathbf{I}^* \mathbf{Q}^r; \quad \text{where } \mathbf{I}^* = \begin{bmatrix} 1 & 0 & 0 \\ 0 & 1 & 0 \\ 0 & 0 & -1 \end{bmatrix} \tag{10}$$

(hence, the "incident" and "reflected" matrices have identical eigenvectors). Then, the (3×3) matrix $\mathbf{R}_\Gamma$ of the reflected coefficients under incident wave of unit amplitude is given by the equation:

$$Z(\mathbf{Q}^i + \mathbf{Q}^r \mathbf{R}_\Gamma) = \mathbf{Z}_\Gamma.(\mathbf{P}^i + \mathbf{P}^r \mathbf{R}_\Gamma).$$

By construction, $R_{\Gamma ri} = R_{r_{Ref}}^{i_{Inc}}$ is the amplitude of the reflected wave r under an incident wave i, where index 1 stands for *SH*, 2 for *SV*, and 3 for *P* waves. By formal inversion, we deduce the reflection coefficients matrix in presence of a surface impedance:

$$\mathbf{R}_\Gamma = -\{\mathbf{Q}^r - (\mathbf{Z}_\Gamma/Z)\mathbf{P}^r\}^{-1}\{\mathbf{Q}^i - (\mathbf{Z}_\Gamma/Z)\mathbf{P}^i\}. \tag{11}$$

3.4. Some limit cases of surface impedance

The reflection matrices $\mathbf{R}_0$ or $\mathbf{R}_\infty$ for free surface condition or perfectly rigid surface condition (i.e. null component of surface motion in the three directions) correspond respectively to the cases $\mathbf{Z}_\Gamma = \mathbf{0}$ or $Z_{\Gamma ii} \to \infty$, $i = 1, 2, 3$. Thus:

$$\mathbf{R}_0 = -(\mathbf{Q}^r)^{-1}\mathbf{Q}^i; \qquad \mathbf{R}_\infty = -(\mathbf{P}^r)^{-1}\mathbf{P}^i.$$

$\mathbf{E}^1$ being eigenvector of $\mathbf{P}$ and $\mathbf{Q}$ matrices, this property also apply to $\mathbf{R}_0$ or $\mathbf{R}_\infty$. This expresses the uncoupling between *SH* waves and *P–SV* waves for free or 3-D rigid boundary conditions. Consequently, SH waves are perfectly reflected, in phase or in phase opposition:

$$(R_0)_{SH}^{SH} = -q_1^{SH_i}/q_1^{SH_r} = -d_3^{SH_i}/d_3^{SH_r} = 1; \qquad (R_\infty)_{SH}^{SH} = -p_1^{SH_i}/p_1^{SH_r} = -1$$

and denoting by $'$ the reduced matrices to the $(\mathbf{e}_2, \mathbf{e}_3)$ components of *SV* and *P* waves, the *P–SV* reflection matrix reads:

$$\mathbf{R}'_0 = -(\mathbf{Q}'^r)^{-1}\mathbf{Q}'^i; \qquad \mathbf{R}'_\infty = -(\mathbf{P}'^r)^{-1}\mathbf{P}'^i.$$

Expression (11) of $\mathbf{R}_\Gamma$ shows that, in presence of $\mathbf{Z}_\Gamma$, the *SH*/*P–SV* uncoupling remains, provided that $\mathbf{e}_1$ (orthogonal to the incidence plane) is an eigenvector of $\mathbf{Z}_\Gamma$. For *SH* and *P–SV* waves to be uncoupled independently of the incidence plane, the horizontal isotropy of $\mathbf{Z}_\Gamma$ (i.e. $Z_{\Gamma 11} = Z_{\Gamma 22}$) is required.

By simple algebraic transformations, $\mathbf{R}_\Gamma$ can be expressed as a combination of $\mathbf{R}_0$ or $\mathbf{R}_\infty$ in the form ($\mathbf{I}$ is the unit matrix):

$$\mathbf{R}_\Gamma = \{\mathbf{I} - (\mathbf{Q}^r)^{-1}(\mathbf{Z}_\Gamma/Z)\mathbf{P}^r\}^{-1}\mathbf{R}_0 + \{\mathbf{I} - ((\mathbf{Z}_\Gamma/Z)\mathbf{P}^r)^{-1}\mathbf{Q}^r\}^{-1}\mathbf{R}_\infty.$$

Thus, for small surface impedance whatever its eigenaxis, the reflection matrix becomes:

$$\mathbf{R}_\Gamma \approx \mathbf{R}_0 + (\mathbf{Q}^r)^{-1}(\mathbf{Z}_\Gamma/Z)\mathbf{P}^r(\mathbf{R}_0 - \mathbf{R}_\infty) \quad \text{when } |\mathbf{Z}_\Gamma/Z| \ll 1.$$

For large surface impedance (in single or several eigendirections) no simple expression can be derived except when $\mathbf{Z}_\Gamma$ is diagonal in the basis $(\mathbf{e}_j)$. In this case (incidence plane containing eigendirection of $\mathbf{Z}_\Gamma$) the *SH*/*P*–*SV* uncoupling remains and enables simple investigation of *mixed* free–rigid boundary conditions corresponding to zero or infinite Z_Γ eigenvalues in the different directions (i.e., either zero stress or motion components).

Exploiting the uncoupling property, the *SH* waves reflect as with free ($Z_{\Gamma 11} = 0$) or rigid ($Z_{\Gamma 11} = \infty$) boundary condition.

As for *P*–*SV* reflection under *mixed* free–rigid boundary conditions, matrices $\mathbf{Q}^a - (\mathbf{Z}_\Gamma/Z)\mathbf{P}^a$, $a = i, r$, are replaced by mixed matrices $\mathbf{M}^a$ whose line i is either the line i of $\mathbf{Q}^a$, if $Z_{\Gamma ii} = 0$, or the line i of $\mathbf{P}^a$, if $Z_{\Gamma ii} = \infty$. From (10) the (2×2) mixed matrices (e.g. $\mathbf{M}'_{0\infty}$ when $Z_{\Gamma 22} = 0, Z_{\Gamma 33} = \infty$) verify:

$$\mathbf{M}'^i_{0\infty} = -\mathbf{M}'^r_{0\infty}; \qquad \mathbf{M}'^i_{\infty 0} = \mathbf{M}'^r_{\infty 0}$$

and therefore, $\mathbf{I}'$ being the unit (2×2) matrix:

$$\mathbf{R}'_{0\infty} = -(\mathbf{M}'^r_{0\infty})^{-1}\mathbf{M}'^i_{0\infty} = \mathbf{I}'; \qquad \mathbf{R}'_{\infty 0} = -(\mathbf{M}'^r_{\infty 0})^{-1}\mathbf{M}'^i_{\infty 0} = -\mathbf{I}'.$$

Consequently, there is no *P*/*SV* mode conversion with *mixed* free–rigid boundary conditions: whatever the incidence angle, *P* or *SV* waves are *perfectly reflected* in a wave of the same nature, in phase when $Z_{\Gamma 22} = 0$ and $Z_{\Gamma 33} = \infty$; in phase opposition in converse case.

In the sequel, the characteristics of the reflection are investigated for (i) isotropic (resp. anisotropic) horizontally resonant surfaces made of oscillators presenting the same (resp. different) characteristics in both horizontal directions and (ii) vertically resonant surface. For simplicity, a single three degree of freedom oscillator is located on Σ and is assumed to behave in each of the three horizontal and vertical directions as a single degree of freedom system as described in Section 2.3.

4. Isotropic horizontally resonant surface

We study isotropic horizontally resonant surface by considering oscillators presenting the same characteristics in both horizontal directions $Z_{\Gamma 11} = Z_{\Gamma 22} = Z_\Gamma$ and having negligible vertical impedance $Z_{\Gamma 33} = 0$. As mentioned previously, this configuration enables uncoupled *SH* and *P*–*SV* waves whatever the incidence plane.

4.1. Reflection of SH waves

Consider an *SH* wave with an incidence angle θ^I. From expression (11) and using the uncoupled wave property, the reflection coefficient of the unique *SH* wave reflected is given by:

$$(R_\Gamma)^{SH}_{SH} = -\frac{d_3^{SH_i} - Z_\Gamma/Z}{d_3^{SH_r} - Z_\Gamma/Z} = \frac{\cos(\theta^I) + Z_\Gamma/Z}{\cos(\theta^I) - Z_\Gamma/Z}.$$

For undamped oscillator, according to impedance expression (5), Z_Γ is purely imaginary at any frequency. Thus:

$$\forall\omega, \qquad \forall\theta^I, \qquad |(R_\Gamma)^{SH}_{SH}| = 1 \quad \text{for } \xi = 0$$

and at low and high frequencies the reflection tends to the free boundary case:

$$(R_\Gamma)^{SH}_{SH} \to (R_0)^{SH}_{SH} = 1 \quad \text{when } \omega \ll \omega_o \text{ or } \omega \gg \omega_o$$

while at the resonant frequencies the reflection tends to the rigid boundary case:

$$(R_\Gamma)^{SH}_{SH} \to (R_\infty)^{SH}_{SH} = -1 \quad \text{when } \omega \to \omega_o.$$

In case of a damped oscillator ($\xi \neq 0$), Z_Γ presenting a negative real part, thus:

$$\forall\omega, \qquad |(R_\Gamma)^{SH}_{SH}| \leq 1 \quad \text{and} \quad (R_\Gamma)^{SH}_{SH} \to \frac{\cos(\theta^I) - \eta/2\xi}{\cos(\theta^I) + \eta/2\xi} \quad \text{when } \omega \to \omega_o$$

while the low and high frequency limits correspond also to free boundary condition. The amplitude and phase variations of $(R_\Gamma)^{SH}_{SH}$ versus frequency are depicted in Fig. 4. The influence of incidence angle and damping are also presented. As expected, the phase changes are mainly concentrated around the oscillator resonance and the amplitude is sensitive to the damping.

Note also the possibility of *vanishing reflected wave* in particular incidences and configurations of oscillator. Indeed, when $\cos(\theta^I) = \eta/2\xi$, $(R_\Gamma)^{SH}_{SH} \to 0$ for $\omega \to \omega_o$ (e.g. see $|R|$ at the resonance $\omega = \omega_o$ in Fig. 4 for $\xi = 5\% = \eta/2$ and $\theta^I = 0$). Thus there is almost no reflected wave and the incident energy is partly dissipated and partly stored in the oscillators in motion: the resonant surface acts as an absorbing layer of *SH* wave. Remark that the damping is essential for this effect, that cannot occur with perfectly elastic oscillators.

The influence of the resonant surface is even more evident when analyzing the surface displacement U_Γ.

$$U_\Gamma = \{1 + (R_\Gamma)^{SH}_{SH}\}U^I = \frac{2U^I}{1 - Z_\Gamma/(Z\cos(\theta^I))}.$$

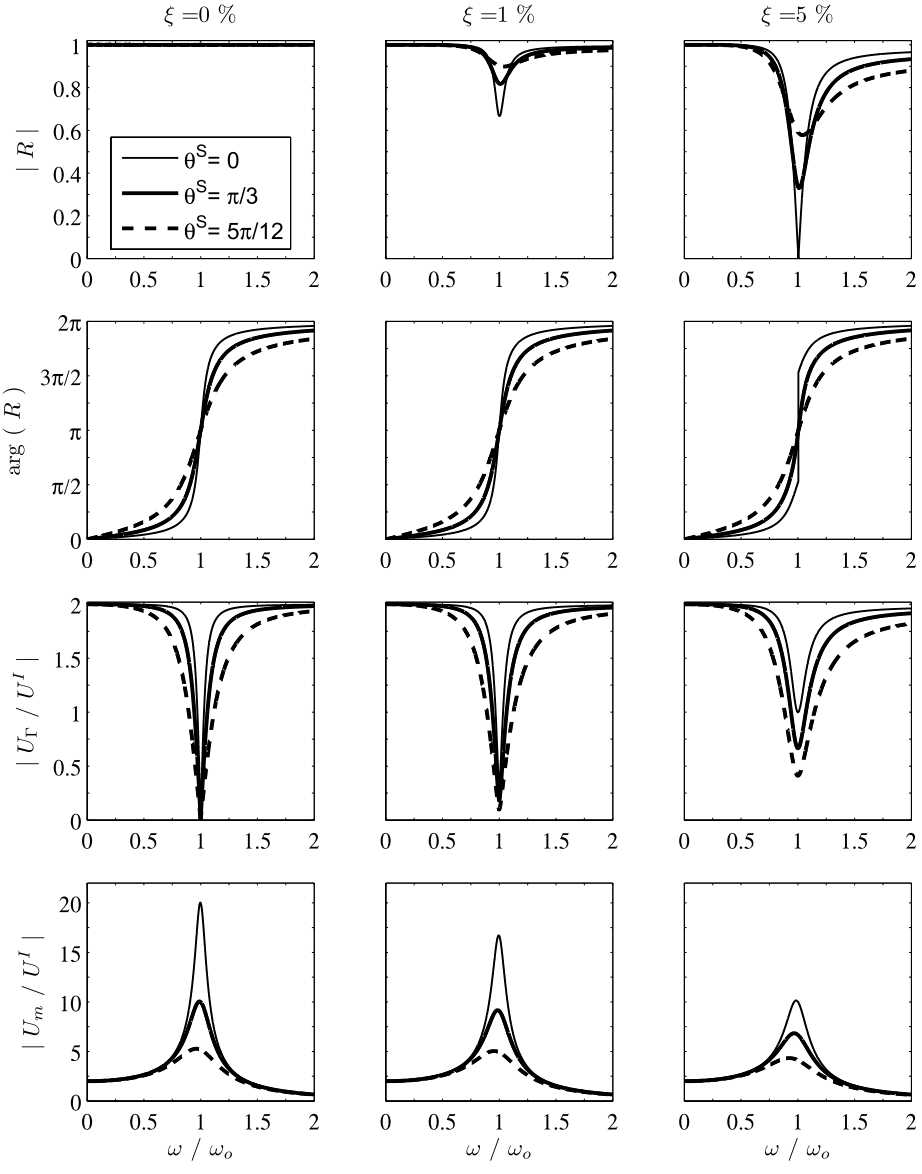

Fig. 4. Isotropic horizontally-resonant surface. Amplitude and phase of the reflection coefficient R of a *SH* wave and amplitude of induced surface displacement U_Γ and oscillators' motion U_m versus dimensionless frequency. Calculations performed at normal and oblique incidences θ^S with $\eta = 0.1$ and different values of oscillator damping.

As shown in Fig. 4, U_Γ is twice the incident displacement when the oscillators are quasi static ($\omega \ll \omega_o$) or in inertial regime($\omega \gg \omega_o$), as expected with a free surface condition and consistently with $|Z_\Gamma/Z| \ll 1$.

At the resonance of perfectly elastic oscillators ($\xi = 0$, $\omega \to \omega_o$), the surface does not move ($U_\Gamma = 0$) as with a rigid surface condition, consistently with $|Z_\Gamma/Z| \to \infty$. For weakly-damped oscillators, the finite contrast of impedances $Z_\Gamma/Z = -\eta/2\xi$ at the resonance leads to $U_\Gamma = U^I 4\xi \cos(\theta^I)/\eta \neq 0$: the impedance condition is no longer analogous to a perfectly rigid surface condition. Note that as the angle of incidence increases, the surface motion decreases significantly. As for the oscillators motion U_m (cf. Section 2.3), simple algebra leads to:

$$U_m = \frac{Z_\Gamma}{Z}\frac{U_\Gamma}{i\eta\omega/\omega_o} = U^I \frac{2\left(1 - i2\xi\frac{\omega}{\omega_o}\right)}{1 - i2\zeta\frac{\omega}{\Omega_o} - \frac{\omega^2}{\Omega_o^2}}$$

where:

$$\Omega_o = \frac{\omega_o}{\sqrt{1 + 2\xi\eta/\cos(\theta^I)}}; \qquad 2\zeta = \frac{2\xi + \eta/\cos(\theta^I)}{\sqrt{1 + 2\xi\eta/\cos(\theta^I)}}.$$

These expressions show that the coupled system oscillates with an apparent damping ζ and an apparent eigenpulsation Ω_o. Remark that U_m is finite at the resonance even though the oscillators are perfectly elastic ($U_m/U_I = 2i\cos(\theta^I)/\eta$ for $\omega = \omega_o$ and $\xi = 0$). The system being non-dissipative, the energy lost by the oscillators is gained by the half-space: the apparent

damping $\eta/2\cos(\theta^l)$ is due to the emission of waves by the oscillators. This is consistent with the fact that when $\eta \ll 1$, i.e. negligible energy turned back into the elastic medium, the effect of the resonant surface is negligible. Further, at normal incidence and for damped oscillators, ratio $\eta/2\xi$ characterizes the competition between the structural damping ξ and the radiative damping $\eta/2$. Interestingly, this energy loss ratio coincides with the impedance ratio Z_Γ/Z at the resonance.

4.2. Reflection P and SV waves

For P or SV wave with an incidence angle θ^l, using expression (11) and the uncoupled wave property, the reflection matrix is given by:

$$\mathbf{R}'_\Gamma = -\{\mathbf{Q}'^r - (\mathbf{Z}'_\Gamma/Z)\mathbf{P}'^r\}^{-1}\{\mathbf{Q}'^i - (\mathbf{Z}'_\Gamma/Z)\mathbf{P}'^i\} \quad \text{with } Z_{\Gamma 22} = Z_\Gamma;\ Z_{\Gamma 33} = 0.$$

From the following expression of matrix $\mathbf{Q}'^r - (\mathbf{Z}'_\Gamma/Z)\mathbf{P}'^r$

$$\begin{bmatrix} 1-2(d_2^{SV})^2 - (Z_\Gamma/Z)d_3^{SV} & 2\dfrac{c_S}{c_P}d_2^P d_3^P - (Z_\Gamma/Z)d_2^P \\ -2d_2^{SV}d_3^{SV} & \dfrac{c_P}{c_S}\left(1-2\left(\dfrac{c_S}{c_P}d_2^P\right)^2\right) \end{bmatrix} \tag{12}$$

and recalling that $\mathbf{Q}'^i - (\mathbf{Z}'_\Gamma/Z)\mathbf{P}'^i = -\mathbf{I}'^*\mathbf{Q}'^r - (\mathbf{Z}'_\Gamma/Z)\mathbf{I}'^*\mathbf{P}'^r$, we deduce by inversion the reflection coefficients in presence of an isotropic horizontally resonant surface. In expressions here below, $d_2 = \sin(\theta^l)$ for the P or SV incident wave and components d_3 stand for d_3^r (i.e. reflected wave).

$$(R_\Gamma)_{SV_r}^{SV_i} = \Delta_S^{-1}\left[(1-2d_2^2)^2 - 4\frac{c_S}{c_P}d_2^2 d_3^{SV} d_3^P + \frac{Z_\Gamma}{Z}d_3^{SV}\right]$$

$$(R_\Gamma)_{P_r}^{SV_i} = 4\Delta_S^{-1}\frac{c_S}{c_P}(1-2d_2^2)d_2 d_3^{SV}$$

$$\Delta_S = (1-2d_2^2)^2 + 4\frac{c_S}{c_P}d_2^2 d_3^{SV} d_3^P - \frac{Z_\Gamma}{Z}d_3^{SV}$$

and

$$(R_\Gamma)_{P_r}^{P_i} = \Delta_P^{-1}\left[-\left(1-2\left(\frac{c_S}{c_P}d_2\right)^2\right)^2 + 4\left(\frac{c_S}{c_P}\right)^3 d_2^2 d_3^{SV} d_3^P + \frac{Z_\Gamma}{Z}d_3^{SV}\right]$$

$$(R_\Gamma)_{SV_r}^{P_i} = 4\Delta_P^{-1}\frac{c_S}{c_P}\left(1-2\left(\frac{c_S}{c_P}d_2\right)^2\right)d_2 d_3^P$$

$$\Delta_P = \left(1-2\left(\frac{c_S}{c_P}d_2\right)^2\right)^2 + 4\left(\frac{c_S}{c_P}\right)^3 d_2^2 d_3^{SV} d_3^P - \frac{Z_\Gamma}{Z}d_3^{SV}.$$

We retrieve the limit cases:

$$\mathbf{R}'_\Gamma \to \mathbf{R}'_0 \quad \text{when } \left|\frac{Z_\Gamma}{Z}\right| \to 0; \qquad \mathbf{R}'_\Gamma \to -\mathbf{I}' \quad \text{when } \left|\frac{Z_\Gamma}{Z}\right| \to \infty.$$

These results are illustrated numerically in Figs. 5 and 6 for incident P waves and in Figs. 7 and 8 for incident SV waves. In both cases, notice in Figs. 5 and 7 the large changes in amplitude and phase of P and SV reflected wave around the resonance, the concerned frequency band being wider for incident SV wave. In quasi static and inertial regimes, the surface condition is analogous to a free surface condition: depending on the incidence angle, the incident P (or SV) wave may be substantially converted into a reflected SV (or P) wave (see Figs. 6 and 8 for $\omega/\omega_o = 0, \xi = 0$). Conversely, for undamped oscillators, a total reflection (i.e. no converted wave) at any angle is observed at the resonance, in accordance with mixed rigid–free condition. For weak damping (see Figs. 6 and 8 for $\omega/\omega_o = 1, \xi = 5\%$), partial conversion occurs, remaining in any case smaller than in free condition. The presence of the critical incidence angle incident SV wave ($\pi/6$ for a Poisson's ratio $\nu = 1/3$) does not modify the general trends. The quasi *vanishing of the total reflected field* for SV wave of normal incidence (Fig. 8 for $\omega/\omega_o = 1$, $\xi = 5\%$) corresponds to the particular situation where $Z_\Gamma/Z = \eta/2\xi = 1$ evoked in Section 4.1, and giving here $(R_\Gamma)_{SV_r}^{SV_i} \simeq 0$ and $(R_\Gamma)_{P_r}^{SV_i} \simeq 0$.

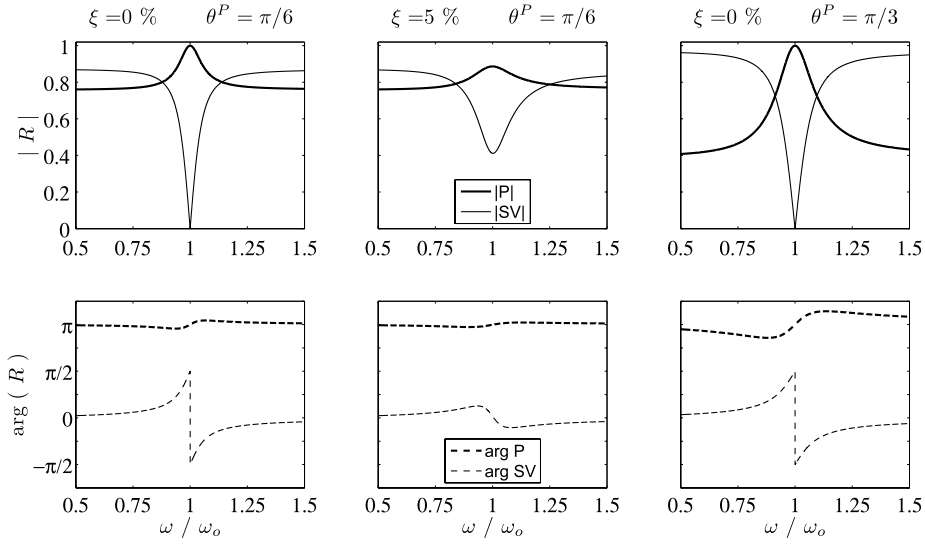

Fig. 5. Isotropic horizontally-resonant surface. Amplitude and phase of the reflection coefficient of a *P* wave versus dimensionless frequency. Calculations performed at oblique incidence θ^P with $\eta = 0.1$, $\nu = 1/3$, and damped or undamped oscillator.

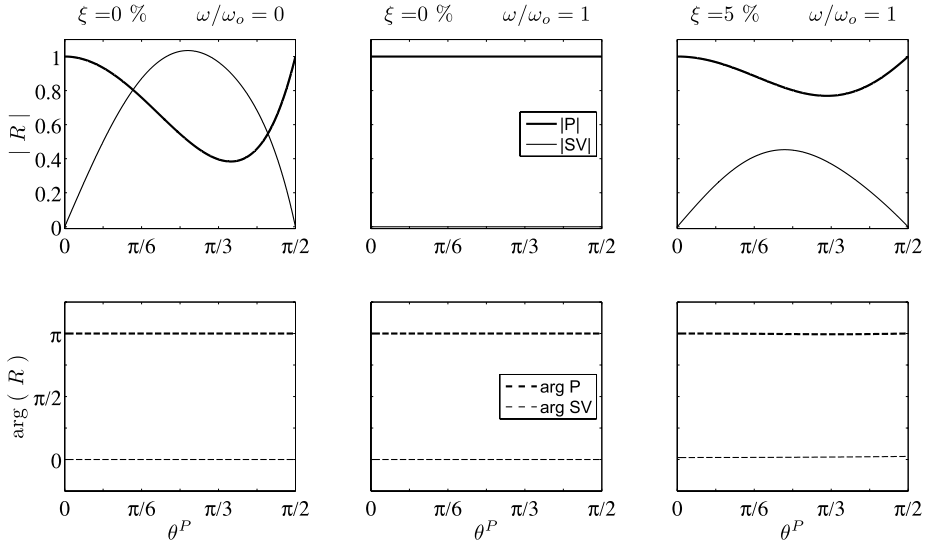

Fig. 6. Isotropic horizontally-resonant surface. Amplitude and phase of the reflection coefficient of a *P* wave versus incidence angle θ^P. Calculations performed in quasi static and resonant regime with $\eta = 0.1$, $\nu = 1/3$, for damped or undamped oscillator.

5. Vertically resonant surface

Another type of isotropic resonant surface is obtained with vertically oscillating resonators presenting negligible impedance in both horizontal directions $Z_{\Gamma 11} = Z_{\Gamma 22} = 0$ and a vertical impedance $Z_{\Gamma 33} = Z_\Gamma$. As mentioned previously, this configuration leads to uncoupled *SH* and *P–SV* waves whatever the incidence plane. Furthermore, the zero horizontal impedance implies the same reflection of *SH* wave as with free boundary condition. Concerning the reflection of *P* and *SV* waves, from expression (11) and the uncoupled wave property, the reflection matrix is given by:

$$\mathbf{R}'_{\Gamma_v} = -\{\mathbf{Q}'^r - (\mathbf{Z}'_\Gamma/Z)\mathbf{P}'^r\}^{-1}\{\mathbf{Q}'^i - (\mathbf{Z}'_\Gamma/Z)\mathbf{P}'^i\} \quad \text{with}\, Z_{\Gamma 22} = 0;\ Z_{\Gamma 33} = Z_\Gamma$$

where here the matrix $\mathbf{Q}'^r - (\mathbf{Z}'_\Gamma/Z)\mathbf{P}'^r$ reads (and similarly for $\mathbf{Q}'^i - (\mathbf{Z}'_\Gamma/Z)\mathbf{P}'^i$):

$$\begin{bmatrix} 1 - 2(d_2^{SV})^2 & 2\dfrac{c_S}{c_P} d_2^P d_3^P \\ -2d_2^{SV} d_3^{SV} - (Z_\Gamma/Z) d_2^{SV} & \dfrac{c_P}{c_S}\left(1 - 2\left(\dfrac{c_S}{c_P} d_2^P\right)^2\right) + (Z_\Gamma/Z) d_3^P \end{bmatrix}. \tag{13}$$

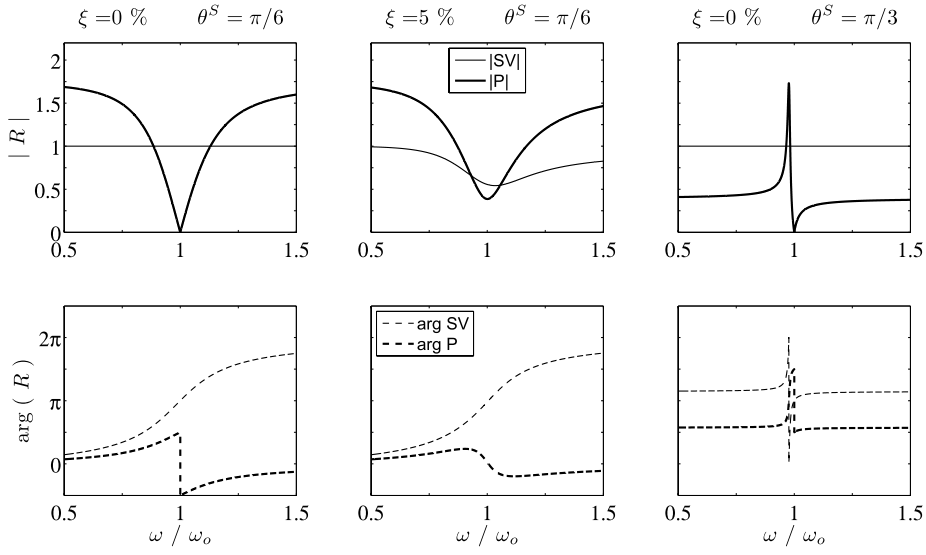

Fig. 7. Isotropic horizontally-resonant surface. Amplitude and phase of the reflection coefficient of a *SV* wave versus dimensionless frequency. Calculations performed at oblique incidence θ^S with $\eta = 0.1$, $\nu = 1/3$, and damped or undamped oscillator.

Then, the reflection coefficients in presence of vertically resonant surface are given by ($d_2 = \sin(\theta^I)$ for the *P* or *SV* incident wave and components d_3 stand for d_3^r, i.e. reflected wave):

$$(R_{\Gamma_v})_{SV_r}^{SV_i} = \Delta_S^{-1}\left[(1-2d_2^2)^2 - 4\frac{c_S}{c_P}d_2^2 d_3^{SV} d_3^P - \frac{Z_\Gamma}{Z}\frac{c_S}{c_P}d_3^P\right]$$

$$(R_{\Gamma_v})_{P_r}^{SV_i} = 4\Delta_S^{-1}\frac{c_S}{c_P}(1-2d_2^2)d_2 d_3^{SV}$$

$$\Delta_S = (1-2d_2^2)^2 + 4\frac{c_S}{c_P}d_2^2 d_3^{SV} d_3^P - \frac{Z_\Gamma}{Z}\frac{c_S}{c_P}d_3^P$$

and

$$(R_{\Gamma_v})_{P_r}^{P_i} = \Delta_P^{-1}\left[-\left(1-2\left(\frac{c_S}{c_P}d_2\right)^2\right)^2 + 4\left(\frac{c_S}{c_P}\right)^3 d_2^2 d_3^{SV} d_3^P - \frac{Z_\Gamma}{Z}\frac{c_S}{c_P}d_3^P\right]$$

$$(R_{\Gamma_v})_{SV_r}^{P_i} = 4\Delta_P^{-1}\frac{c_S}{c_P}\left(1-2\left(\frac{c_S}{c_P}d_2\right)^2\right)d_2 d_3^P$$

$$\Delta_P = \left(1-2\left(\frac{c_S}{c_P}d_2\right)^2\right)^2 + 4\left(\frac{c_S}{c_P}\right)^3 d_2^2 d_3^{SV} d_3^P - \frac{Z_\Gamma}{Z}\frac{c_S}{c_P}d_3^P.$$

Again, we have the limit cases:

$$\mathbf{R}'_{\Gamma_v} \to \mathbf{R}'_0 \quad \text{when} \quad \left|\frac{Z_\Gamma}{Z}\right| \to 0; \qquad \mathbf{R}'_{\Gamma_v} \to \mathbf{I}' \quad \text{when} \quad \left|\frac{Z_\Gamma}{Z}\right| \to \infty.$$

Results are presented in Figs. 9 and 10 for incident *P* waves and in Figs. 11 and 12 for incident *SV* waves. They call for similar general comments – about the variation versus frequency, the importance of damping and the influence of incidence angle – as for horizontal isotropic surface. Nevertheless the inversion of axis of the free and impedance condition leads to reflected fields notably different in both cases. Note also in this configuration, the possibility of a quasi *vanishing of the total reflected field* (i.e. $(R_{\Gamma v})_{SV_r} \simeq 0$ and $(R_{\Gamma v})_{P_r} \simeq 0$) around the resonance $\omega/\omega_o = 1$ (giving $Z_\Gamma/Z = -\eta/2\xi$):

- for *P* wave of normal incidence for the particular value $\eta/2\xi = c_P/c_S$.
- for *SV* wave of $\pi/4$ incidence ($d_2 = 1/\sqrt{2}$) for the particular value $\eta/2\xi = \sqrt{2}$.

In both cases the damped resonator layer acts as a (quasi-)perfect absorbing surface.

6. Horizontally anisotropic resonant surface

Focus now on anisotropic horizontally-resonant surface made of resonators having a single direction of oscillation along $\mathbf{e}_\alpha$ as shown in Fig. 13. Thus, expressed in the basis ($\mathbf{e}_\alpha$, $\mathbf{e}_\beta$, $\mathbf{e}_3$) the impedance matrix is diagonal with the principal values:

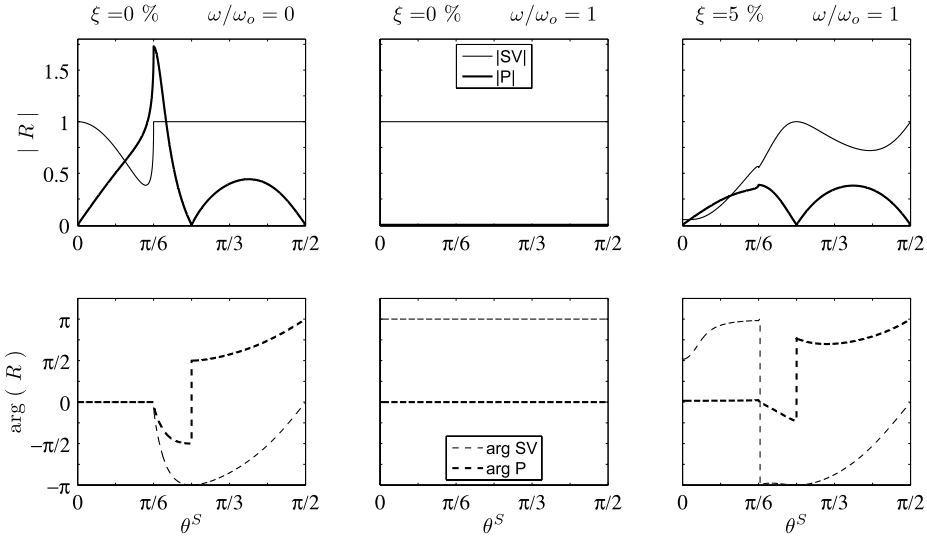

Fig. 8. Isotropic horizontally-resonant surface. Amplitude and phase of the reflection coefficient of a *SV* wave versus incidence angle θ^S. Calculations performed in quasi static and resonant regime with $\eta = 0.1$, $\nu = 1/3$, for damped or undamped oscillator.

$Z_{\Gamma\alpha\alpha} = Z_\Gamma, Z_{\Gamma\beta\beta} = 0, Z_{\Gamma 33} = 0$. When the incidence plane contains the principal direction of $\mathbf{Z}_\Gamma$, *SH* waves and *P–SV* waves are uncoupled and we obtain the same reflection scheme as for isotropic horizontally resonant surface. However, if the incidence plane differs from the impedance eigenaxes, the three waves are coupled and new situations arise. These atypical phenomena are investigated for incident *SH* waves of normal incidence and of oblique incidence.

6.1. Reflection of out of impedance axis waves of normal incidence

Denote by α the angle between $\mathbf{e}_\alpha$ and $\mathbf{e}_1$, so that *SH* waves are polarized in the resonant direction for $\alpha = 0$. Making the usual change of basis, the impedance matrix expressed in the basis $(\mathbf{e}_j)$ defined by the incidence plane and Γ reads:

$$\mathbf{Z}_\Gamma = Z_\Gamma \begin{bmatrix} \cos^2(\alpha) & -\sin(2\alpha)/2 & 0 \\ -\sin(2\alpha)/2 & \sin^2(\alpha) & 0 \\ 0 & 0 & 0 \end{bmatrix}.$$

Thus, for normally incident wave ($d_2 = \sin(\theta^I) = 0$), matrices involved in the reflection matrix (11), e.g. $\mathbf{Q}^r - (\mathbf{Z}_\Gamma/Z)\mathbf{P}^r$ read:

$$\mathbf{Q}^r - (\mathbf{Z}_\Gamma/Z)\mathbf{P}^r = \begin{bmatrix} 1 - \dfrac{Z_\Gamma}{Z}\cos^2(\alpha) & \dfrac{Z_\Gamma}{Z}\sin(2\alpha)/2 & 0 \\ \dfrac{Z_\Gamma}{Z}\sin(2\alpha)/2 & 1 - \dfrac{Z_\Gamma}{Z}\sin^2(\alpha) & 0 \\ 0 & 0 & \dfrac{c_P}{c_S} \end{bmatrix}.$$

Simple algebra leads to the following reflection coefficients of normal wave incident in a plane out of axis of the impedance matrix:

$$\mathbf{R}''_{\Gamma_\alpha} = \frac{1}{1 - \frac{Z_\Gamma}{Z}} \begin{bmatrix} 1 + \dfrac{Z_\Gamma}{Z}\cos(2\alpha) & \dfrac{Z_\Gamma}{Z}\sin(2\alpha) \\ -\dfrac{Z_\Gamma}{Z}\sin(2\alpha) & 1 - \dfrac{Z_\Gamma}{Z}\cos(2\alpha) \end{bmatrix}; \qquad (R_{\Gamma_\alpha})^P_P = 1$$

where $\mathbf{R}''_{\Gamma_\alpha}$ denotes the reduced reflection matrix to the $(\mathbf{e}_1, \mathbf{e}_2)$ components of *SH* and *SV* waves (since both *S* waves are normal, we will use here the notation SH_1 for *SH* wave polarized in direction $\mathbf{e}_1$ and SH_2 for *SV* wave polarized in direction $\mathbf{e}_2$). As expected in this configuration, normal *P* waves are uncoupled with *SH* normal waves. However, an unusual SH_1–SH_2 coupling appears.

Obviously, in the limit of small impedance, one obtains classical reflection with free boundary condition:

$$\mathbf{R}''_{\Gamma_\alpha} \to \mathbf{I}' \quad \text{when} \quad \left|\frac{Z_\Gamma}{Z}\right| \to 0.$$

Now, for large impedance, that corresponds to the resonance of undamped oscillator ($\omega/\omega_o = 1, \xi = 0$), the reflection is atypical:

$$\mathbf{R}'_{\Gamma_\alpha} \to \begin{bmatrix} -\cos(2\alpha) & -\sin(2\alpha) \\ \sin(2\alpha) & \cos(2\alpha) \end{bmatrix} \quad \text{when} \quad \left|\frac{Z_\Gamma}{Z}\right| \to \infty.$$

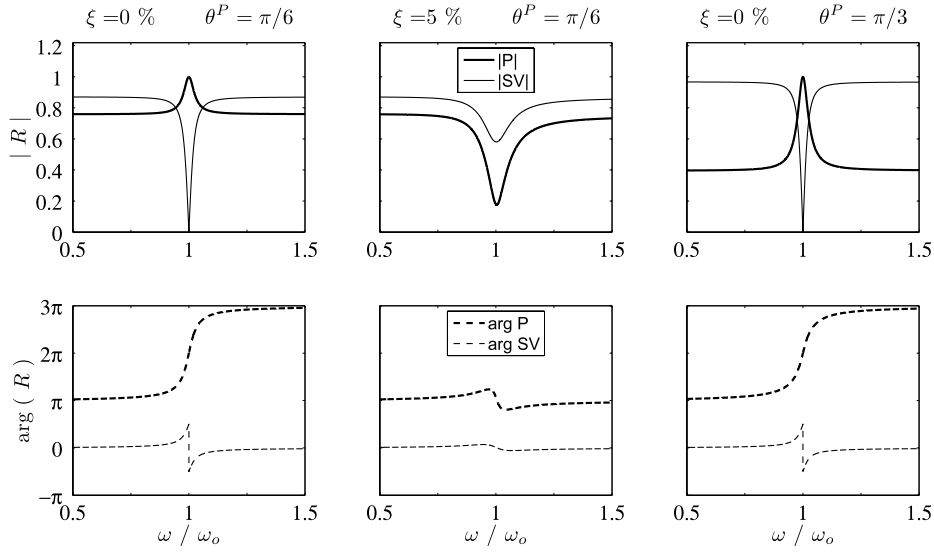

Fig. 9. Vertically resonant surface. Amplitude and phase of the reflection coefficient of a *P* wave versus dimensionless frequency. Calculations performed at oblique incidence θ^S with $\eta = 0.1$, $\nu = 1/3$, and damped or undamped oscillator.

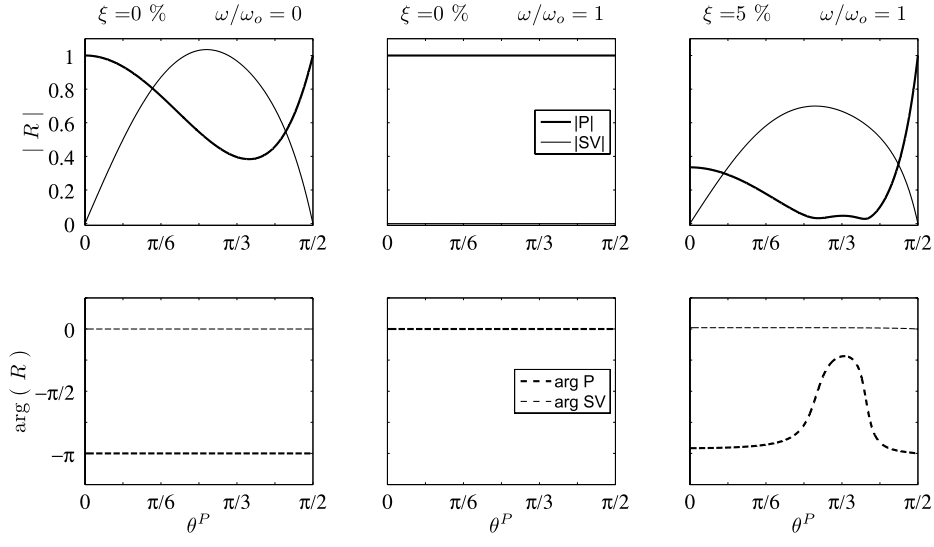

Fig. 10. Vertically resonant surface. Amplitude and phase of the reflection coefficient of a *P* wave versus incidence angle θ^P. Calculations performed in quasi static and resonant regime with $\eta = 0.1$, $\nu = 1/3$, for damped or undamped oscillator.

Thus, when $\alpha = 0$ (i.e. incident SH_1 wave polarized in the resonant direction $\mathbf{e}_\alpha$ and incidence plane perpendicular to this direction) the SH_1 motion induces resonance and the reflection corresponds to rigid condition ($R = -1$). Conversely, an incident SH_2 motion does not trigger resonance and the reflection corresponds to free surface condition ($R = 1$). Remark that SH_1 and SH_2 roles are inverted for incidence plane containing the direction of oscillation ($\alpha = \pi/2$).

In the general case $\alpha \neq 0$, a *SH* wave is reflected in a SH_1 and a SH_2. Note that when $\alpha = \pm\pi/4$, there is a *complete conversion* of incident SH_1 into reflected SH_2 and reciprocally. This means that the resonant surface acts as a *mechanical depolarizer* of *SH* wave.

An alternative way to describe this depolarization phenomenon is to project a normally incident *S* wave polarized along $\mathbf{e}_S$ (oriented with an angle ϕ relatively to the resonant direction $\mathbf{e}_\alpha$) on the eigenaxes ($\mathbf{e}_\alpha$, $\mathbf{e}_\beta$) of the surface impedance: $\mathbf{u}^i = u\mathbf{e}_S = u^i_\alpha \mathbf{e}_\alpha + u^i_\beta \mathbf{e}_\beta$ where $u^i_\alpha = u\cos(\phi)$ and $u^i_\beta = u\sin(\phi)$. To respect the boundary conditions (i.e. zero α-component of motion and zero β-component of stress) we have $u^r_\alpha = -u^i_\alpha$ and $u^r_\beta = u^i_\beta$. Consequently:

$$\mathbf{u}^r.\mathbf{u}^i = u^2(-\cos(\phi)\mathbf{e}_\alpha.\mathbf{e}_S + \sin(\phi)\mathbf{e}_\beta.\mathbf{e}_S) = -u^2\cos(2\phi).$$

The reflected field is therefore orthogonal to the incident field when the polarization makes an angle of $\phi \pm \pi/4$ with the resonant direction.

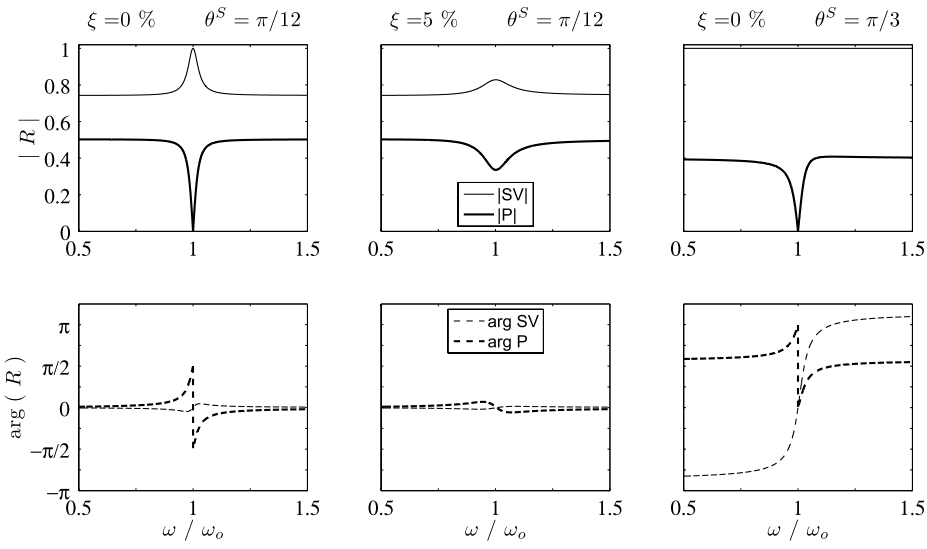

Fig. 11. Vertically resonant surface. Amplitude and phase of the reflection coefficient of a *SV* wave versus dimensionless frequency. Calculations performed at oblique incidence θ^S with $\eta = 0.1$, $\nu = 1/3$, and damped or undamped oscillator.

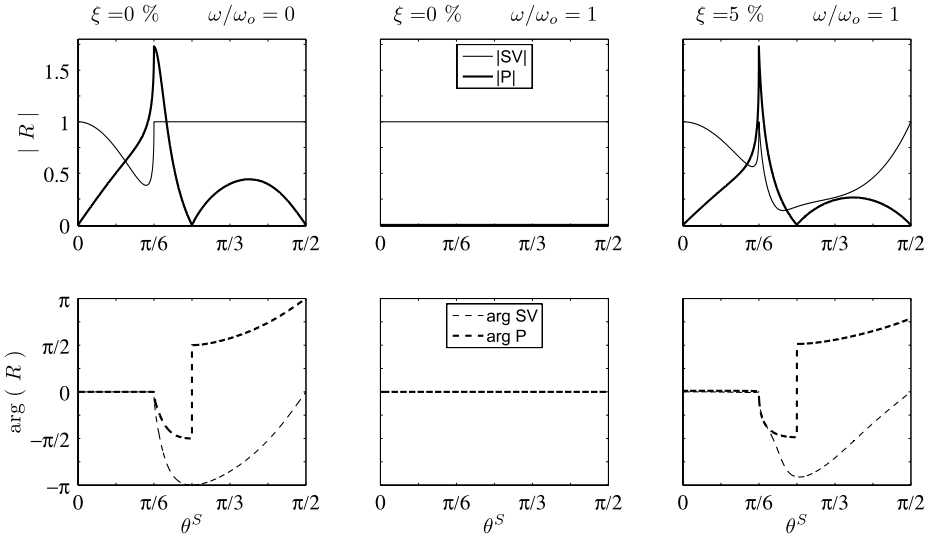

Fig. 12. Vertically resonant surface. Amplitude and phase of the reflection coefficient of a *SV* wave versus incidence angle θ^S. Calculations performed in quasi static and resonant regime with $\eta = 0.1$, $\nu = 1/3$, for damped or undamped oscillator.

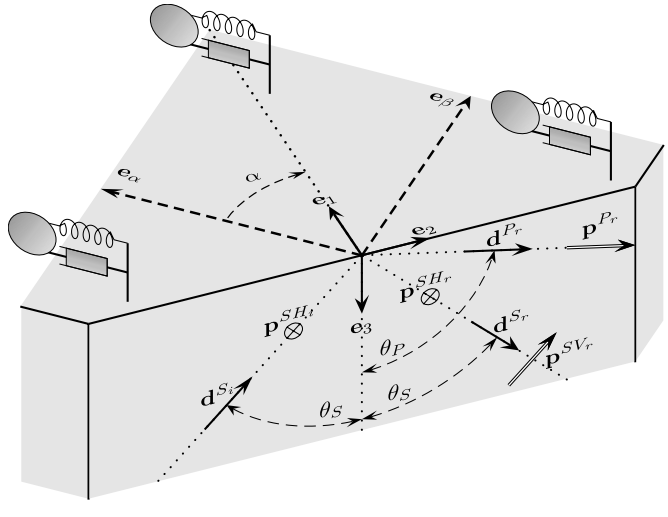

Fig. 13. Horizontally anisotropic resonant surface. Oblique incident *SH* wave which polarization makes an angle α with the resonant direction.

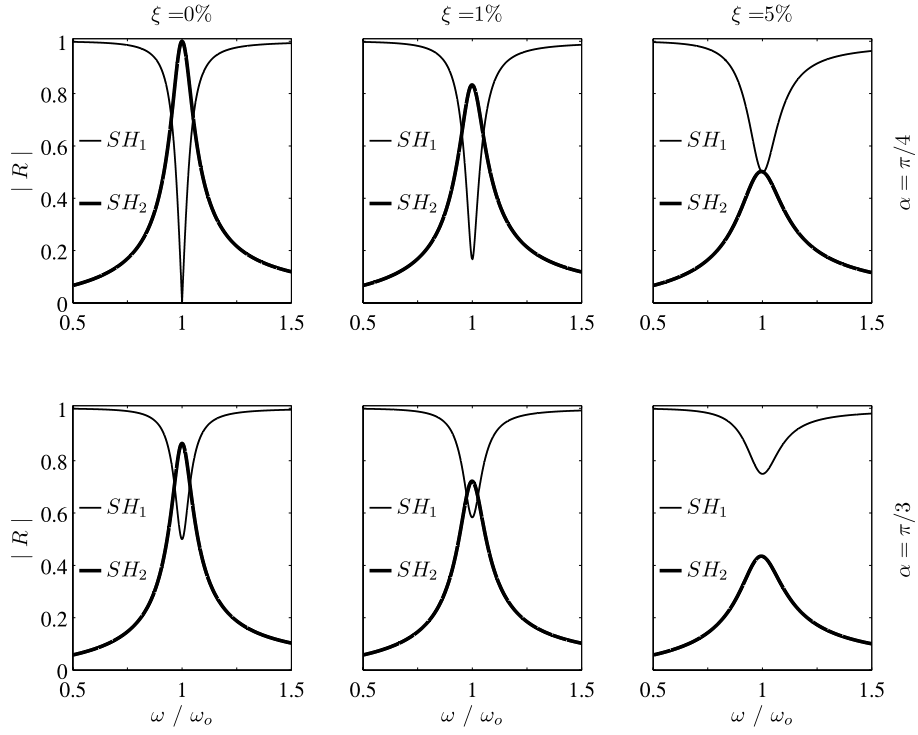

Fig. 14. Anisotropic horizontally-resonant surface; SH_1 wave of normal incidence which polarization makes an angle α with the resonant direction. Amplitude of the reflected SH_1 and SH_2 waves versus dimensionless frequency. Calculations performed with $\eta = 0.1$, for damped or undamped oscillator with $\alpha = \pi/4$ and $\pi/3$.

At the resonance of weakly-damped oscillators ($\omega/\omega_o = 1, \xi \neq 0$), the reflection matrix reads:

$$\mathbf{R}''_{\Gamma_\alpha} \simeq \frac{1}{1+\frac{\eta}{2\xi}} \begin{bmatrix} 1-\dfrac{\eta}{2\xi}\cos(2\alpha) & -\dfrac{\eta}{2\xi}\sin(2\alpha) \\ \dfrac{\eta}{2\xi}\sin(2\alpha) & 1+\dfrac{\eta}{2\xi}\cos(2\alpha) \end{bmatrix}.$$

Thus, provided that $\frac{\eta}{2\xi} > 1$ the depolarization phenomena still exist for incident SH_1 wave polarized in the directions $\alpha_p = \pm\frac{1}{2}\arccos\frac{2\xi}{\eta}$ so that $(\mathbf{R}''_{\Gamma_\alpha})_{11} = 0$ (or equivalently for incident SH_2 with plane wave defined by $\alpha+\pi/2 = \pm\frac{1}{2}\arccos\frac{2\xi}{\eta}$). The two α_p directions are not perpendicular, but are symmetric with regard to $\mathbf{e}_\alpha$. The depolarized wave is partially reflected with the reflection factor: $\sqrt{\left(\frac{\eta}{2\xi}-1\right)/\left(\frac{\eta}{2\xi}+1\right)}$. For incident plane angles $\alpha \neq \alpha_p$, the depolarization is partial, nevertheless the top surface motion is always oriented (quasi-) perpendicularly to the resonant direction.

Finally, the complex character of the impedance, associated with the SH_1–SH_2 coupling, induces the fact that the top surface motions in both directions are generally ($\omega/\omega_o \neq 1$) out of phase. Hence, the top surface particulate motion takes an ellipsoidal form.

The frequency-dependent depolarization effects are illustrated in Fig. 14 that underlines the significant influence of frequency, damping and of incidence plane angle.

6.2. Reflection of out of impedance axis SH waves of oblique incidence

The same resolution approach applies for oblique incidence in an incidence plane out of impedance axis. However, in that case there is a full coupling of *SH*, *SV* and *P* modes. Indeed, consider for example an out of impedance axes *SH* wave (Fig. 13). The full coupling relies on the fact that the *SH* wave puts in motion the resonators, that induce in turn surface stresses in both directions ($\mathbf{e}_1$, $\mathbf{e}_2$). The reflected *SH* wave can only balance the stresses along $\mathbf{e}_1$. To cancel the stress along $\mathbf{e}_2$ an oblique reflected *SV* wave is at least required. Due to the normal stress induced by this *SV* wave an oblique *P* wave is also reflected.

In this situation no simple algebraic expressions can be derived. Thus, we focus on obliquely-incident *SH* waves and present in Fig. 15 the numerical results of reflection amplitude according to the frequency and the angle of the incidence plane. The drastic change and the great diversity of the reflected fields according to these parameters are clearly evidenced. Note for instance the possibility of incident oblique *SH* wave ($\theta = \pi/6$) to be totally reflected into *P* and *SV* wave (case $\xi = 0\%, \alpha \simeq \pi/6$) or to be totally reflected into non-homogeneous *P* and homogeneous *SH* wave (case $\theta = \pi/4$).

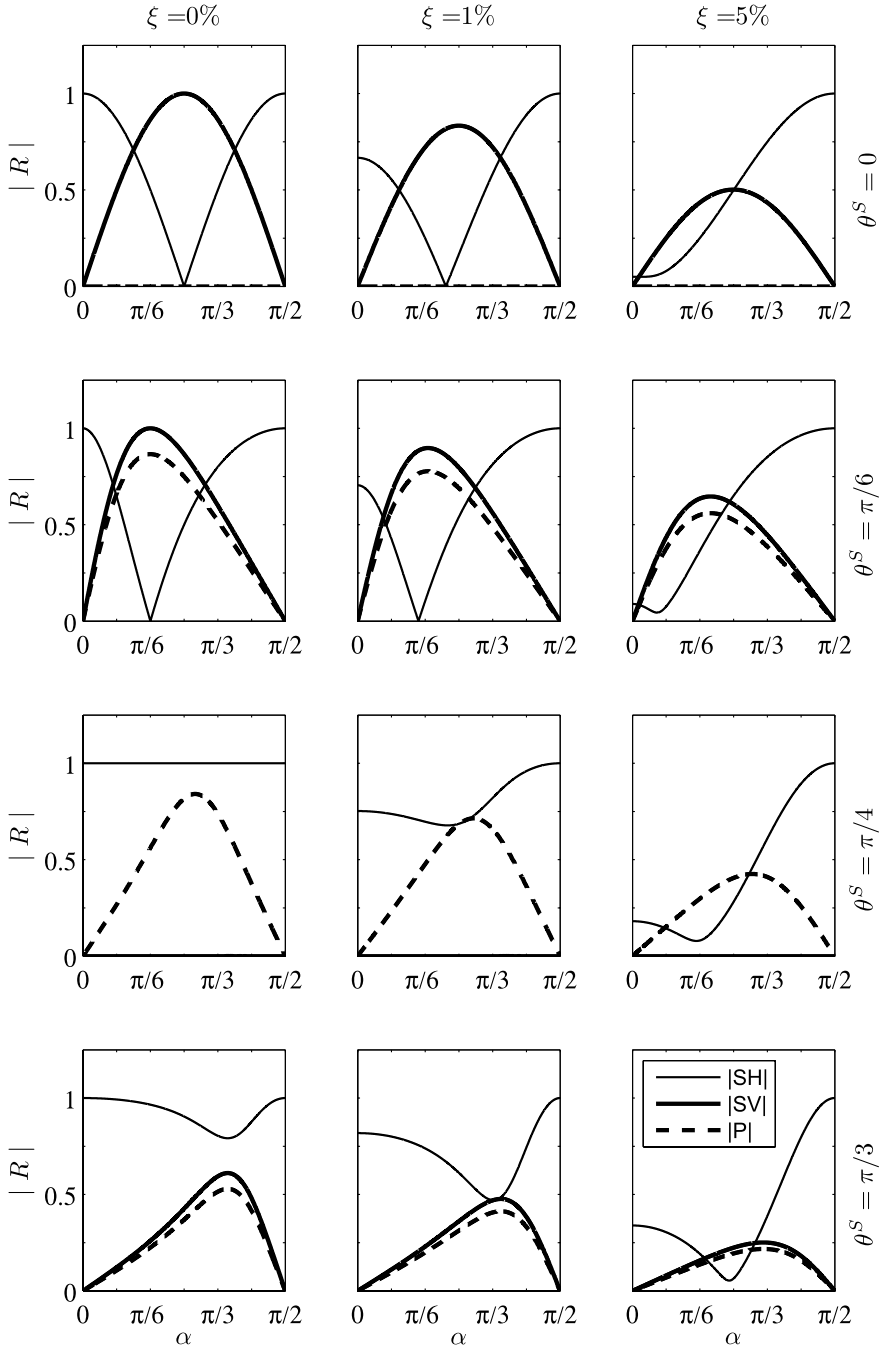

Fig. 15. *SH* wave in θ^S-incidence on an anisotropic horizontally-resonant surface. *SH* polarization makes an angle α with the resonant direction. Calculations performed with $\nu = 1/3$ and $\eta = 0.1$.

7. Conclusion

The very specificity of resonant surfaces lies in the coincidence of frequency range inducing (i) long wavelength dynamics in the supporting layer and (ii) local dynamics of the periodically distributed oscillators. In this sense, resonant surfaces may be seen as a 2D-version of "meta-material" see e.g. [13–15]. The "inner-dynamics" on the surface induces resonance amplification that leads to particular boundary conditions expressed in terms of frequency dependent impedance. This phenomenon and its formulation depart from the usual conditions considered to address corrugated surfaces—e.g. [16–18].

Let us remind that the equivalent impedance approach requires a scale separation. Thus, its validity is limited to the frequency range where the wavelengths are larger than the spatial period. Note also that when the scale separation is well marked, periodic or non-periodic spatial distribution lead to similar macroscopic behavior.

The systematic study of unconventional reflections in presence of a resonant surface underlines the common properties related to the "inner-dynamics" and peculiarities associated with given configurations. The main features of a resonant surface can be summarized as follows:

- the effect is concentrated around the eigenfrequency of the oscillators;
- the efficiency can be estimated through three parameters, i.e. scale separation ε, mass ratio η and oscillator damping ξ;
- as a consequence of resonance, the boundary condition is switched from quasi-free surface condition, to quasi-rigid surface condition in the resonance frequency range and in the resonance direction only.

Numerous configurations can be contemplated by combining oscillators. In particular, isotropic or anisotropic resonant surfaces can be obtained, that open the possibility of unusual mixed (quasi-) free and (quasi-) rigid boundary conditions in different directions (unrealizable with an elastic upper layer). According to the nature of the incident field and the configuration of the resonant surface, the most notable effects identified around the resonant frequency are:

1. a drastic change of *P* and *SV* waves conversion;
2. the full depolarization of normally-incident shear waves;
3. the conversion of *SH* waves into *P* and *SV* waves;
4. the possibility for the whole reflected field to vanish.

In this study, the resonators are reduced to simple oscillators. For practical applications, this simple case can be extended with similar principles to more complex cases, for instance using slender beams or plates as resonator (made of the same or different material from the supporting layer). Finally, the identification of the nature of the reflected field according to the resonator characteristics enables to consider the design of resonant surfaces in order to modify the reflection properties in a prescribed way. Further experimental works are in progress in this direction in order to evidence the actual effect of resonant surface in real configurations.

References

[1] C. Boutin, P. Roussillon, Wave propagation in presence of oscillators on the free surface, International Journal of Engineering Science 44 (2006) 180–204.
[2] A. Wirgin, P.-Y. Bard, Effects of building on the duration and amplitude of ground motion in Mexico city, Bulletin of the Seismological Society of America 86 (3) (1996) 914–920.
[3] D. Clouteau, D. Aubry, Modification of ground motion in dense urban areas, Journal of Computational Acoustics 9 (4) (2001) 1659–1675.
[4] C. Boutin, P. Roussillon, Assessment of the urbanization effect on seismic response, Bulletin of the Seismological Society of America 94 (1) (2004) 251–268.
[5] V.A. Eremeyev, H. Altenbach, On the eigenfrequencies of an ordered system of nanoobjects, in: R. Pyrz, J.C. Rauhe (Eds.), IUTAM Symposium on Modelling Nanomaterials and Nanosystems, 2009, pp. 123–132.
[6] E. Sánchez-Palencia, Non-homogeneous Media and Vibration Theory, in: Lecture Notes in Physics, vol. 127, Springer-Verlag, Berlin, 1980.
[7] J.-L. Auriault, C. Boutin, C. Geindreau, Homogenization of Coupled Phenomena in Heterogenous Media, in: ISTE, John Wiley & Sons Inc., 2009.
[8] G. Bouchitté, A. Lidouh, P. Suquet, Homogénéisation de frontière pour la modélisation du contact entre un corps déformable non linéaire et un corps rigide, Comptes Rendus de l'Academie des Sciences, Serie I (Mathematique) 313 (13) (1991) 967–972.
[9] R. Weaver, Multiple-scattering theory for mean responses in a plate with sprung masses, Journal of the Acoustical Society of America 101 (6) (1997) 3466–3474.
[10] C. Soize, A model and numerical method in the medium frequency range for vibroacoustic predictions using theory of structural fuzzy, Journal of the Acoustical Society of America 94 (2) (1993) 849–865.
[11] M. Strasberg, D. Feit, Vibration damping of large structures induced by attached small resonant structures, Journal of the Acoustical Society of America 99 (1) (1996) 335–344.
[12] C.L. Holloway, E. Kuester, Impedance-type boundary conditions for a periodic interface between a dielectric and a highly conducting medium, IEEE Transactions on Antennas and Propagation 48 (10) (2000) 1660–1672.
[13] P. Sheng, X. Zhang, Z. Liu, C. Chan, Locally resonant sonic materials, Physica B: Condensed Matter 338 (2003) 201–205.
[14] Z. Liu, C.T. Chan, P. Sheng, Analytic model of phononic crystals with local resonance, Physical Review B: Condensed Matter and Materials Physics 71 (2005) 014103.
[15] J. Auriault, C. Boutin, Long wavelength inner-resonance cut-off frequencies in elastic composite materials, International Journal of Solids and Structure 49 (2012) 3269–3281.
[16] E.J. Sabina, J. Willis, Scattering of *SH* waves by a rough half-space of arbitrary slope, Geophysical Journal of the Royal Astronomical Society 42 (2) (1975) 685–703.
[17] D. Berman, J. Perkins, Rayleigh method for scattering from random and deterministic interfaces, Journal of the Acoustical Society of America 88 (1990) 1032–1044.
[18] J. Nevard, J.B. Keller, Homogenization of rough boundaries and interfaces, SIAM Journal of Applied Mathematics 57 (6) (1997) 1660–1686.